

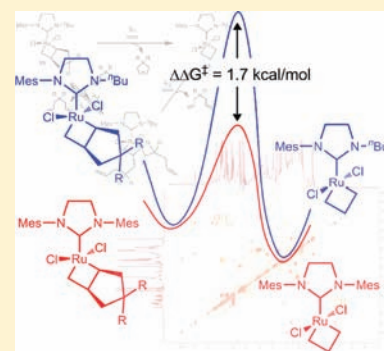
# Probing the Origin of Degenerate Metathesis Selectivity via Characterization and Dynamics of Ruthenacyclobutanes Containing Variable NHCs

Benjamin K. Keitz and Robert H. Grubbs\*

Arnold and Mabel Beckman Laboratories of Chemical Synthesis, Division of Chemistry and Chemical Engineering, California Institute of Technology, Pasadena, California 91125, United States

Supporting Information

**ABSTRACT:** The preparation of new phosphonium alkylidene ruthenium metathesis catalysts containing N-heterocyclic carbenes (NHCs) that result in a preference for degenerate metathesis is described. The reaction of the catalysts with ethylene or substrates relevant to ring-closing metathesis (RCM) produced ruthenacyclobutanes that could be characterized by cryogenic NMR spectroscopy. The rate of  $\alpha/\beta$  methylene exchange in ethylene-only ruthenacycles was found to vary widely between ruthenacycles, in some cases being as low as  $3.97\text{ s}^{-1}$  at  $-30\text{ }^{\circ}\text{C}$ , suggesting that the NHC plays an important role in degenerative metathesis reactions. Attempts to generate RCM-relevant ruthenacycles resulted in the low-yielding formation of a previously unobserved species, which we assign to be a  $\beta$ -alkyl-substituted ruthenacycle. Kinetic investigations of the RCM-relevant ruthenacycles in the presence of excess ethylene revealed a large increase in the kinetic barrier of the rate-limiting dissociation of the cyclopentene RCM product compared with previously investigated catalysts. Taken together, these results shed light on the degenerate/productive selectivity differences observed for different metathesis catalysts.



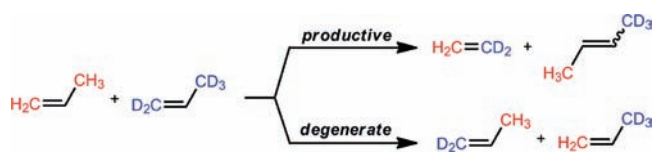
## INTRODUCTION

Olefin metathesis continues to evolve as one of the most effective methods for the construction of new carbon–carbon bonds.<sup>1,2</sup> This evolution has been facilitated by the development and intense mechanistic study of the catalysts responsible for this transformation.<sup>3</sup> Accordingly, metathesis has found applications in a wide range of fields including polymer chemistry,<sup>4</sup> organic synthesis,<sup>5</sup> biochemistry,<sup>6</sup> and green chemistry.<sup>7</sup>

Implicit in many olefin metathesis reactions is the presence of degenerate or nonproductive events. For instance, in the self cross-metathesis reaction of propylene, a productive reaction would result in the formation of 2-butene, while a degenerate reaction would reform propylene. As the degenerate reaction reproduces the starting olefin, it can be reliably studied only via isotopic crossover experiments (Scheme 1). Elegant experiments from a multitude of research groups using early metal catalysts and selectively labeled olefins have established that degenerate metathesis occurs approximately an order of magnitude faster than productive metathesis and appears to be due to a propagating alkylidene species.<sup>8</sup> To date, analogous studies have not been performed with modern, well-defined metathesis catalysts based on ruthenium, despite the importance of degenerate events to catalyst efficiency.

Our group recently reported a study of degenerate events taking place during RCM of an isotopically labeled diethyl diallylmalonate (**1**) in which we discovered the surprising effect of NHC structure on a catalyst's propensity to perform either productive or degenerate turnovers.<sup>9</sup> The results of this study

Scheme 1. Productive and Degenerate Metathesis of Propylene



validated the importance of degenerate metathesis events and their subsequent effect on a catalyst's efficiency and stability. Furthermore, we also recently established that selectivity for degenerate metathesis may actually be *beneficial* in some applications, such as the ethenolysis of methyl oleate.<sup>10</sup> In addition, in the case of group VI catalysts, degenerate events have been shown to play a critical role in enantioselective metathesis reactions.<sup>11</sup>

For ruthenium metathesis catalysts, the effect of ligand structure on initiation and stability has been well-documented.<sup>12,13</sup> This knowledge has allowed the development of increasingly sophisticated catalysts. However, much less is known about the effect of ligand structure on processes that occur within a complex catalytic cycle such as RCM. This lack of understanding has made it difficult to rationalize the behavior of catalysts asked to conduct increasingly challenging transformations. Recently, the situation

Received: August 2, 2011

Published: September 15, 2011

has been remedied by the development of rapidly initiating catalysts and their ability to form ruthenacyclobutanes efficiently at low temperature, which has facilitated the solution-phase study of previously inaccessible metathesis intermediates by our group<sup>14</sup> as well as Piers and co-workers<sup>15,16</sup> (Figure 1). By analyzing these intermediates and using a combination of kinetics and kinetic modeling, the Piers laboratory was able to determine the activation energies for the fundamental steps along the productive RCM pathway.<sup>17</sup>

While the above results will undoubtedly facilitate the development of more efficient catalysts, we sought to utilize them as a basis to establish the effect of the NHC on each elementary reaction in the RCM catalytic cycle. Specifically, we wanted to correlate these effects with the preference for degenerate selectivity and thereby acquire a more intimate understanding of the role of the NHC in establishing the selectivity for either degenerate or productive olefin metathesis. Herein we report our progress toward this goal.

## RESULTS AND DISCUSSION

In view of our interest in degenerate metathesis, catalysts incorporating NHCs known to give lower selectivity for productive

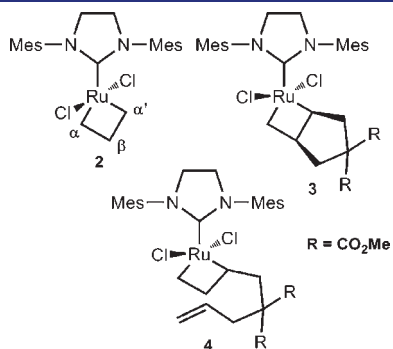
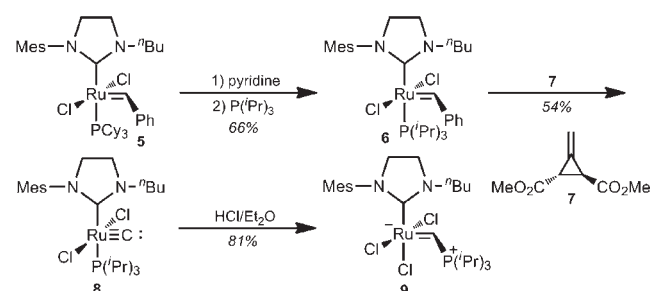
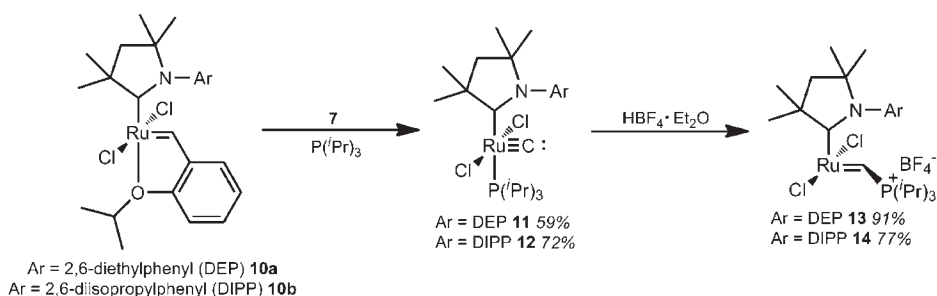


Figure 1. Previously observed ruthenacycles relevant to RCM.

### Scheme 2. Synthesis of Phosphonium Alkylidene Catalyst 9



### Scheme 3. Synthesis of Catalysts 13 and 14

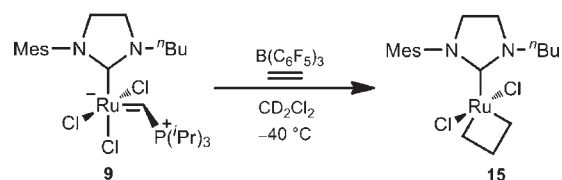


metathesis in the RCM of **1** were selected for study.<sup>9</sup> Thus, we started with previously reported catalyst **5** and performed a phosphine exchange in order to expedite the formation of ruthenacycles.<sup>15c,18</sup> Subsequent reaction with Feist's ester (**7**) yielded carbide **8**, which we then protonated with HCl in Et<sub>2</sub>O to afford the desired phosphonium alkylidene complex **9** in good yield (Scheme 2).<sup>19</sup>

Similarly, the reaction of the cyclic alkylamino carbene (CAAC) catalysts of type **10** with **7** in the presence of 1 equiv of P(iPr)<sub>3</sub> yielded carbides **11** and **12**, which were then protonated in a manner analogous to **8** to obtain the desired complexes **13** and **14** (Scheme 3). Notably, this result demonstrates that phosphonium alkylidene complexes may be obtained from Hoveyda-type parent complexes in situations where the corresponding phosphine precursor is synthetically inaccessible.

With **9**, **13**, and **14** in hand, we next attempted the preparation of ethylene-derived ruthenacycles, as even these simple metallacycles can provide insight into the influence of the NHC ligand. Gratifyingly, complete conversion to metallacycle **15** was observed after 3 h at −40 °C when **9** was exposed to B(C<sub>6</sub>F<sub>5</sub>)<sub>3</sub> and 1 atm ethylene (Scheme 4). Consistent with analogous complexes, **15** displayed an upfield resonance at −2.4 ppm characteristic of the hydrogen on the β-carbon of the ruthenacycle. We found compound **15** to be stable for several days at −78 °C, and it could be fully characterized by <sup>1</sup>H NMR spectroscopy and 2D techniques such as <sup>1</sup>H–<sup>1</sup>H correlation spectroscopy (COSY) [see the Supporting Information (SI)].<sup>20</sup> A rotational Overhauser effect spectroscopy (ROESY) spectrum taken at −60 °C (Figure 2) displayed cross-peaks indicative of chemical exchange between the protons on the α and β carbons of the ruthenacycle. Curiously, cross-peaks were observed only between α-H and β-H and not between α'-H and β-H. Although interesting, this situation is not unprecedented and appears to be a result of asymmetry in the NHC affecting the ruthenacycle.<sup>15b</sup> We next attempted to measure the rate constant for exchange (*k*<sub>15-Ex</sub>) between the α and β protons using exchange spectroscopy (EXSY). Unfortunately, the presence of a minor peak overlapping with the α-H resonance in **15** resulted in irreproducible measurements. However, switching to a magnetization transfer technique allowed us

### Scheme 4. Generation of an Ethylene-Only Ruthenacycle from 9



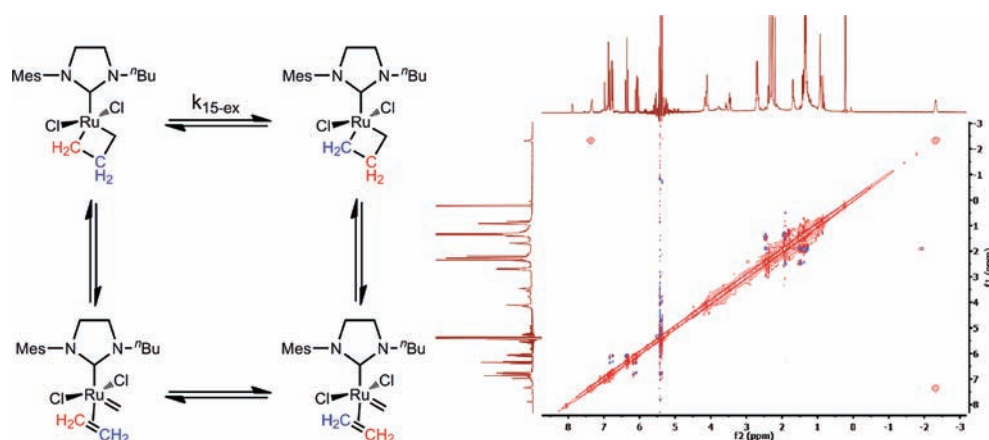


**Figure 2.** (left) Mechanism of ruthenacycle methylene exchange and (right) ROESY spectrum at  $-60\text{ }^{\circ}\text{C}$  with cross-peaks indicative of chemical exchange.

**Scheme 5. Generation of Ethylene-Only Ruthenacycles from 13 and 14**

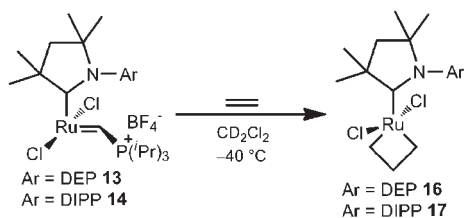


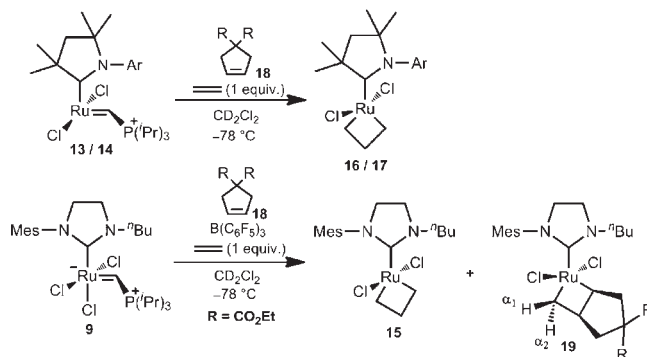
**Table 1. Ruthenacycle  $\alpha/\beta$  Methylene Exchange Rates for All Complexes**

complex	$T\text{ (}^{\circ}\text{C)}$	exchange rate constants ( $\text{s}^{-1}$ )
15	$-60$	10.5
16	$-30$	3.97
17	$-60$	1.48

to obtain a  $k_{15\text{-Ex}}$  value of  $10.5\text{ s}^{-1}$  at  $-60\text{ }^{\circ}\text{C}$  (see the SI). This value is in good agreement with previous reports for ruthenacycles incorporating 1,3-dimesitylimidazolidine-2-ylidene ( $\text{H}_2\text{IMes}$ ), such as **2**.<sup>21</sup> An Eyring plot over the temperature range from  $-40$  to  $-80\text{ }^{\circ}\text{C}$  (Figure S10 in the SI) yielded the values  $\Delta H^{\ddagger} = 10.1 \pm 0.5\text{ kcal mol}^{-1}$  and  $\Delta S^{\ddagger} = -5.7 \pm 2.2\text{ cal mol}^{-1}\text{ K}^{-1}$ .

Similar to the case of **9** above, the reactions of **13** and **14** with an excess of ethylene under similar conditions cleanly yielded ruthenacycles **16** and **17** (Scheme 5).<sup>22</sup> Characterization of **16** was performed according to the procedure described above, but a ROESY NMR spectrum at  $-60\text{ }^{\circ}\text{C}$  showed only a nuclear Overhauser effect (NOE) between the  $\alpha$ -H and  $\beta$ -H; no evidence of chemical exchange was observed. In fact, chemical exchange via ROESY and magnetization transfer was not observed until the temperature was raised to  $-30\text{ }^{\circ}\text{C}$ ! Measurement of the exchange rate constant via magnetization transfer yielded an extraordinarily low value of  $3.97\text{ s}^{-1}$  at  $-30\text{ }^{\circ}\text{C}$  (Table 1). Thus, in comparison with the values for other catalysts (e.g., **2** and **15**),  $k_{16\text{-Ex}}$  is lower, even at higher temperatures. This effect could be observed qualitatively: the ruthenacycle

**Scheme 6. Synthesis of Substituted Ruthenacycles from 9, 13, and 14**



resonances in **16** were still sharp at  $-30\text{ }^{\circ}\text{C}$ , whereas the same resonances in **15** were significantly broadened as a result of chemical exchange (Figure S9). In contrast to **16**, a ROESY spectrum of ruthenacycle **17** taken at  $-60\text{ }^{\circ}\text{C}$  showed evidence of chemical exchange, albeit with a relatively low rate constant (Table 1). Although it is difficult to extract definitive conclusions from such dramatic changes in methylene exchange rates, particularly at the low temperatures under investigation, the extent to which the NHC can affect even the simplest of metathesis reactions is still noteworthy. Furthermore, the low rate of exchange in **16**, even at relatively high temperatures, suggests that similar complexes may be viable targets for crystallographic characterization of metathesis-relevant ruthenacycles.

Having established the feasibility of forming simple ruthenacycles with **9**, **13**, and **14**, we turned to the preparation and characterization of ruthenacycles relevant to RCM. With an approach similar to that used by the Piers' laboratory, **9**, **13**, and **14** were reacted with cyclopentene **18** (produced by RCM of **1**) in the presence of 1 equiv of ethylene (Scheme 6).<sup>15c,17</sup> Unfortunately, under a variety of conditions, **13** and **14** reacted to give the ethylene-only ruthenacycles **16** and **17**, respectively. Such an observation is consistent with the known preference of catalysts containing these NHCs to propagate as methylenes species in catalytic reactions (e.g., in ethenolysis),<sup>23</sup> but it is nevertheless surprising that no other ruthenacycles were observed.<sup>24</sup> In contrast

to **13** and **14**, when **9** was reacted with **18** and 1 equiv of ethylene at  $-78\text{ }^{\circ}\text{C}$ , substituted metallacycle **19** was observed, albeit in very low yield (ca. 29%). In all cases, a significant amount of the parent ethylene-only metallacycle **15** was also formed (ca. 21% yield). Despite the low yield of **19**, we were able to characterize the metallacycle resonances fully by  $^1\text{H}-^1\text{H}$  COSY and found them to be consistent with previous literature reports (see below).<sup>15c,17</sup> To our surprise, ROESY spectra taken at a variety of different temperatures ( $-40$  to  $-70\text{ }^{\circ}\text{C}$ ) and mixing times (up to 600 ms) displayed no evidence of chemical exchange apart from the methylene exchange in **15**. This is in contrast to compound **3**, which exhibits a number of dynamic processes, including exchange between  $\alpha^1$  and  $\alpha^2$  resonances and exchange between **3** and free cyclopentene (Scheme 7).

When the mixture of **15** and **19** was warmed to  $-40\text{ }^{\circ}\text{C}$  for 2 h, a new peak appeared in the metallacycle region of the NMR spectrum. At first, we believed this peak to be the result of ring opening of **19** followed by trapping with ethylene, a process that was observed by Piers (e.g., to form **4**).<sup>17</sup> However, several lines of evidence suggest that an entirely different intermediate is formed under our conditions. First, Piers and co-workers found that ring-opened ruthenacycle **4** was formed only at low temperatures (below  $-60\text{ }^{\circ}\text{C}$ ), whereas the formation of the observed structure occurred only at higher temperatures ( $-40\text{ }^{\circ}\text{C}$ ).

#### Scheme 7. Unobserved Exchange Processes in **19**

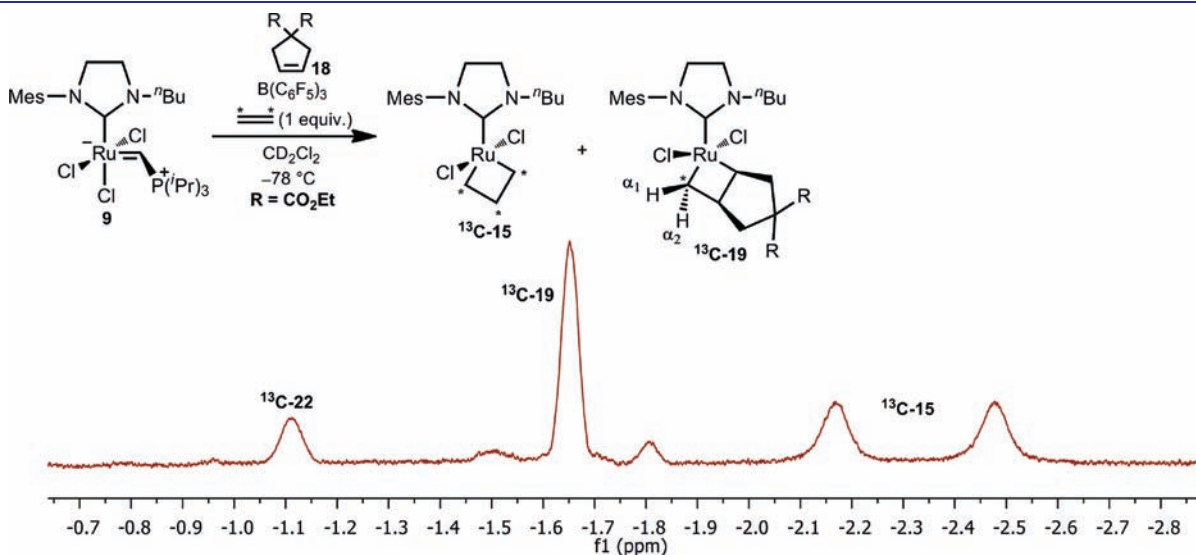
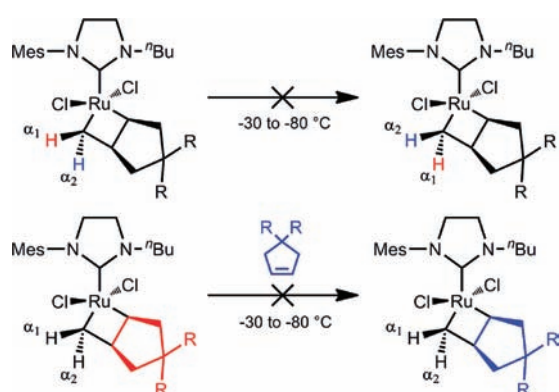


**Figure 3.** (top) Generation of substituted ruthenacycles using  $^{13}\text{C}$ -ethylene and (bottom) NMR spectrum showing resonances for  $^{13}\text{C}$ -**15** ( $-2.2$  and  $-2.5\text{ ppm}$ ),  $^{13}\text{C}$ -**19** ( $-1.65\text{ ppm}$ ), and  $^{13}\text{C}$ -**22** ( $-1.1\text{ ppm}$ ).

Second and more importantly, substitution at  $\alpha'$  should create a set of diastereotopic  $\beta$ -H resonances. Thus, if a structure analogous to **4** were correct, there would have been two separate resonances, which were not observed. In order to characterize this new species and confirm the identity of **19**, compound **9** was reacted with **18** in the presence of  $^{13}\text{C}$ -labeled ethylene (Figure 3 top). The resulting NMR spectrum taken at  $-60\text{ }^{\circ}\text{C}$  (Figure 3 bottom) showed that only one of the three  $\beta$ -H resonances (at  $-2.4\text{ ppm}$ ) was split by virtue of being bound to a  $^{13}\text{C}$ -enriched nucleus.<sup>25</sup> This corresponds to the ethylene-only ruthenacycle **15**. The other two  $\beta$ -H resonances remained as singlets, indicating that these protons must have come from substrate **18**. These data rule out the presence of a ruthenacycle resulting from ring opening of **19** and trapping of the resulting alkylidene with ethylene. The extremely low concentration of the unknown ruthenacycle and its relatively short  $T_2$  prevented us from establishing its structure by heteronuclear 2D NMR spectroscopy (e.g., HSQC, HMB).<sup>26</sup> However, we were able to obtain a  $^1\text{H}-^1\text{H}$  COSY spectrum at  $-90\text{ }^{\circ}\text{C}$  (Figure 4) that provided some insight into the structure of the unknown species.

The COSY data confirmed our original assignments of **15** and **19** and also showed cross-peaks for the unknown species that suggest the following: (1) The  $\beta$  carbon of the ruthenacycle is substituted with an alkyl group, as shown by a small correlation observed in the alkyl region. (2) The  $\beta$ -H is adjacent to a  $^{13}\text{C}$ -enriched nucleus, as shown by a correlation in the  $\alpha/\alpha'$ -H ruthenacycle region that was split into a doublet. (3) The  $\alpha$  carbon of the ruthenacycle is also alkyl-substituted, as shown by a downfield correlation consistent with those for other  $\alpha$ -substituted ruthenacycles. On the basis of these results, we propose structure **22** in Scheme 8 for the unknown ruthenacycle. If this structure is correct, it would be the first observation of a  $\beta$ -substituted ruthenacycle that is not part of a ring system. However, as a caveat, it must be noted that it is currently not clear what role (if any) a structure such as **22** plays in either productive or nonproductive metathesis. The formation of **22** would require ring opening of **19** to generate an alkylidene followed by trapping with diene  $^{13}\text{C}$ -**1** instead of ethylene (Scheme 8). This would obviously require that diene  $^{13}\text{C}$ -**1** be present in solution.



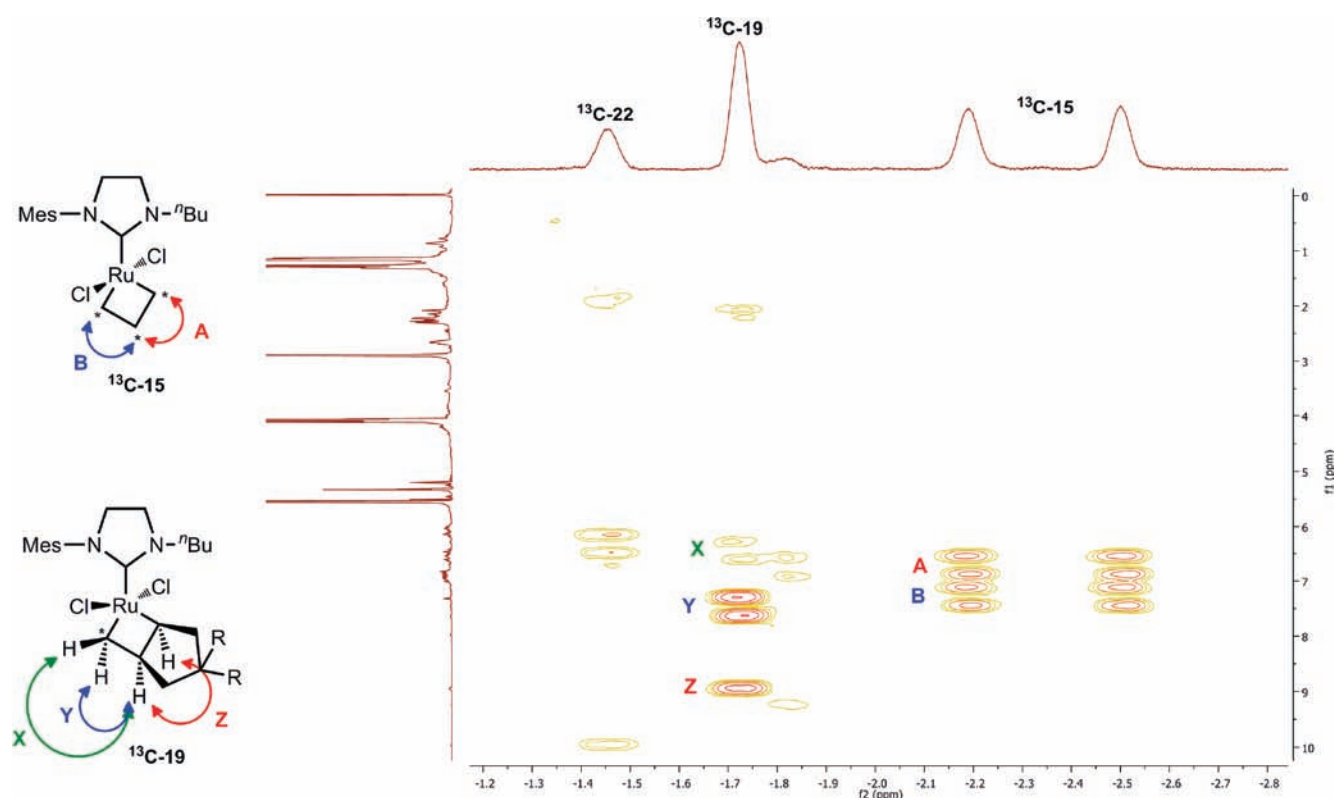
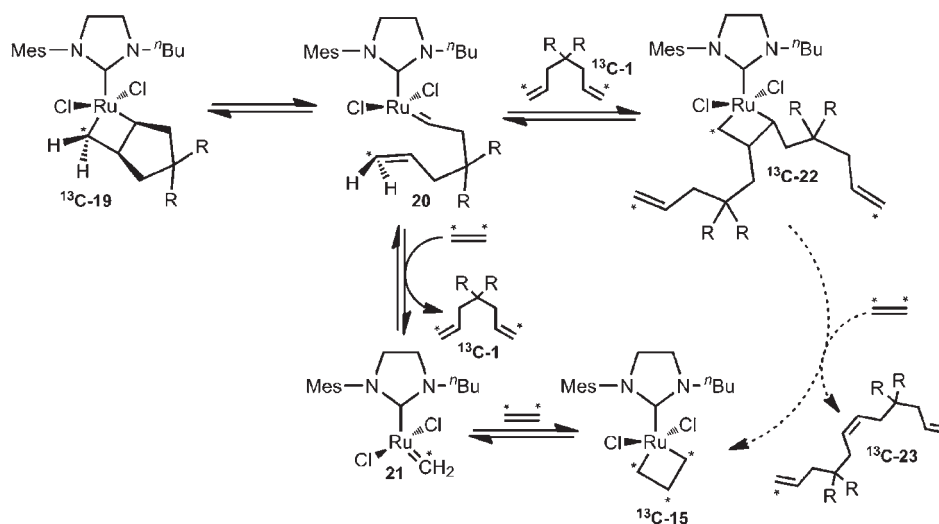


**Figure 4.**  $^1\text{H}$ - $^1\text{H}$  COSY spectrum of the ruthenacycle region for the  $^{13}\text{C}$ -labeled ruthenacycle mixture at  $-90^\circ\text{C}$  in  $\text{CD}_2\text{Cl}_2$ . The assignments of A and B in  $^{13}\text{C}$ -15 are arbitrary since there was not enough spectroscopic data to distinguish the two. The X, Y, and Z assignments were confirmed by 2D NOESY.

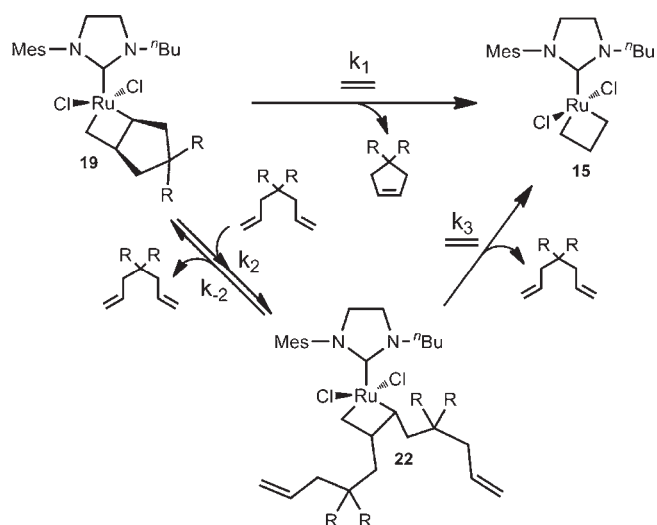
**Scheme 8. Proposed Formation of Diene 1 and Ruthenacycle 22 from 19 and Ethylene (Dashed Lines Represent a Possible Process That Was Not Observed<sup>29</sup>)**



A heteronuclear single-quantum correlation (HSQC) and  $^{13}\text{C}$  NMR spectrum confirmed the presence of  $^{13}\text{C}$ -1, but we were unable to establish its concentration reliably because of the overlap of several species in the same region of the 1D  $^1\text{H}$  NMR spectrum (see the Supporting Information).<sup>27</sup> However, reaction of 9 with diene 1 in place of 18 yielded the same three ruthenacycle resonances, although the relative concentrations of the various

ruthenacycles were largely unchanged relative to previous experiments. The structure shown for 22 is consistent with all of our spectroscopic data, but unfortunately, its low concentration prevented us from establishing its identity with full confidence.<sup>28</sup> Furthermore, we were also unable to find conditions where 22 did not form, a fact that tremendously complicated our kinetic investigations. Nevertheless, we decided to probe the transformation

**Scheme 9. Kinetic Model for the Conversion of 19 to 15 and 22 in the Presence of Excess Ethylene**



from **19** to **15** in the hope of providing some insight into the effect of the NHC on more advanced ruthenacycle kinetics.

Exposure of an isotopically labeled mixture of  $^{13}\text{C}$ -**19** and  $^{13}\text{C}$ -**22** to an excess of ethylene (1 atm) at  $-60\text{ }^\circ\text{C}$  for 6 h revealed only a marginal decrease in the intensity of the corresponding resonances. This result is in contrast to what the Piers' laboratory observed with **3**, which was consumed within hours under similar conditions. Perhaps more surprising was the low rate of reaction of ruthenacycle  $^{13}\text{C}$ -**15**, which showed almost no significant washing out of the  $^{13}\text{C}$  label. Again, this is in contrast to catalyst **2** formed from  $^{13}\text{C}$ -labeled ethylene, where the isotopic label was completely washed out within hours, albeit at the higher temperature of  $-50\text{ }^\circ\text{C}$ .<sup>14b</sup> In a separate experiment, increasing the temperature of the reaction of **19** with excess ethylene to form **15** at  $-40\text{ }^\circ\text{C}$  resulted in clean first-order kinetics that could be monitored on a more manageable time frame using NMR spectroscopy. However, a closer inspection of the kinetic data revealed a second first-order process that appeared to be occurring at short reaction times (Figure S17). We believe that this additional process was the result of an equilibrium between **19** and **22** at early reaction times. Indeed, a time-course plot of the concentrations of **15**, **19**, and **22** revealed a slight increase in the concentration of **22** followed by a leveling off at later reaction times (Figure S18). This result confirmed that there are two processes leading to the decrease in the concentration of **19**: (1) the direct reaction to form **15** with release of **18** and (2) an apparent equilibrium reaction to form **22** followed by conversion of **22** into **15** (Scheme 9).<sup>29</sup> An analogous sequence of reactions was observed by Piers under certain conditions, albeit with a different intermediate (**4**). Modeling of the simplified series of reactions shown in Scheme 9 using COPASI<sup>30</sup> allowed the kinetic parameters  $k_1$ ,  $k_2$ ,  $k_{-2}$ , and  $k_3$  to be determined (Table S5).<sup>31,32</sup> Comparison of the  $k_1$  values obtained for **19** and **3**<sup>17</sup> revealed a stark contrast between the reactivities of the two compounds. For example, at  $-60\text{ }^\circ\text{C}$ , the  $k_1$  value obtained for **3** was  $7 \times 10^{-4}\text{ s}^{-1}$ , whereas the value for **19** ( $7.3 \times 10^{-6}\text{ s}^{-1}$ ) was 2 orders of magnitude smaller. An Eyring plot using the  $k_1$  values for **19** over a  $20\text{ }^\circ\text{C}$  temperature range yielded a value of  $19.0 \pm 0.5\text{ kcal mol}^{-1}$  for  $\Delta H^\ddagger$ , which is ca.  $3\text{ kcal mol}^{-1}$  higher than the corresponding

value for **3** ( $16.2\text{ kcal mol}^{-1}$ ). The  $\Delta S^\ddagger$  values obtained for the two systems were roughly the same ( $8.5 \pm 2.3\text{ cal mol}^{-1}\text{ K}^{-1}$  for **19** vs  $3.6\text{ cal mol}^{-1}\text{ K}^{-1}$  for **3**).

Although we urge caution in extrapolating these results to behavior under catalytic conditions and normal operating temperatures, this fundamental transformation in the RCM cycle is clearly much more difficult for **19** than for **3**, which may partially explain the lower activities typically associated with complexes of this type. Furthermore, since loss of the cyclopentene product from **19** or **3** appears to be the rate-determining step in the ring-closing direction, we speculate that the relative increase in the height of this barrier for **19** may allow for more degenerate turnovers to occur before a productive turnover can be completed.<sup>16</sup> This would account for the observation that catalysts containing structurally similar NHCs select for degenerate turnovers during RCM.<sup>8</sup> Finally, the observation of  $^{13}\text{C}$ -**1** in solution suggests that ring opening of the cyclopentene RCM product is facile and perhaps that the kinetic preference for ring closing over ring opening is catalyst-dependent.<sup>33</sup>

## CONCLUSION

In summary, several new phosphonium alkylidene ruthenium metathesis catalysts incorporating different NHCs have been prepared and used to generate ruthenacycles with the goal of rationalizing degenerate metathesis selectivity. In the case of ethylene-only ruthenacycles, the rate of exchange of  $\alpha$  and  $\beta$  methylene protons was found to vary considerably across the series of catalysts. With traditional NHCs, the exchange rate was largely consistent with previously reported complexes, while incorporation of a CAAC with DEP as the nitrogen substituent resulted in severe attenuation of the exchange rate to the point where exchange was not observed until the temperature was increased to  $-30\text{ }^\circ\text{C}$ . Because of this relatively low exchange rate, one can envision that crystallographic characterization of this complex (or analogous ones) may be possible. However, subtle changes in ligand architecture can alter the ruthenacycle exchange rate, and by extension, the metathesis selectivity and activity. This was demonstrated by the remarkable increase in exchange rate upon substituting DEP with DIPP as the nitrogen substituent on the CAAC ligand. These results demonstrate the significant changes that can occur in even the simplest of metathesis reactions as a result of changes in the NHC structure.

Our attempts to form RCM-relevant ruthenacycles resulted in the formation of a previously unobserved ruthenacycle that we believe to be the first acyclic  $\beta$ -alkyl-substituted ruthenacycle. Such a structure is consistent with all of our spectroscopic data, but its low concentration placed a definitive identification currently out of our technical reach. Nevertheless, this structure plays an important role in ruthenacycle kinetics under an atmosphere of excess ethylene. Our kinetic investigations revealed that the rate-limiting dissociation of the cyclopentene RCM product from the ruthenium center has a much higher energy barrier in comparison with previously reported complexes. Since the majority of the steps along the RCM pathway appear to be reversible, this higher barrier may allow more degenerate turnovers to occur at the expense of productive ones. At the very least, it provides an additional rationale for the generally inferior performance of metathesis catalysts containing *N*-aryl/*N*-alkyl NHCs in comparison with those possessing *N*-aryl/*N*-aryl NHCs.

Finally, these studies further illuminate the subtle role that the NHC plays in ruthenium-catalyzed olefin metathesis, thus

validating efforts to fine-tune ruthenium catalysts for specific applications via manipulation of this ligand.

## ■ ASSOCIATED CONTENT

**S Supporting Information.** Detailed experimental procedures, NMR spectra, and kinetic analysis. This material is available free of charge via the Internet at <http://pubs.acs.org>.

## ■ AUTHOR INFORMATION

### Corresponding Author

rhg@caltech.edu

## ■ ACKNOWLEDGMENT

We thank Ms. Taylor Lenton, Ms. Rachel Klet, Mr. Ian Tonks, Dr. Edward Weintrob, and Prof. John Bercaw for assisting with high-vacuum Schlenk techniques and quantitative gas transfers. Dr. Jay Labinger and Prof. Anna Wenzel are thanked for helpful discussions. Dr. David VanderVelde is acknowledged for assisting with NMR experimentation and analysis. This work was financially supported by the NIH (NIH SR01GM031332-27), the NSF (CHE-1048404), and the NDSEG (fellowship to B.K.K.). Instrumentation facilities on which this work was carried out were supported by NIH RR027690. Materia, Inc., is thanked for its donation of metathesis catalysts.

## ■ REFERENCES

- (1) (a) Fürstner, A. *Angew. Chem., Int. Ed.* **2000**, *39*, 3013. (b) Trnka, T. M.; Grubbs, R. H. *Acc. Chem. Res.* **2001**, *34*, 18. (c) Schrock, R. R. *Chem. Rev.* **2002**, *102*, 145. (d) Schrock, R. R.; Hoveyda, A. H. *Angew. Chem., Int. Ed.* **2003**, *42*, 4592. (e) Astruc, D. *New J. Chem.* **2005**, *29*, 42.
- (2) Grubbs, R. H. *Handbook of Metathesis*; Wiley-VCH: Weinheim, Germany, 2003.
- (3) (a) Vougioukalakis, G.; Grubbs, R. H. *Chem. Rev.* **2010**, *110*, 1746. (b) Samojłowicz, C.; Bieniek, M.; Grela, K. *Chem. Rev.* **2009**, *109*, 3708.
- (4) (a) Leitgeb, A.; Wappel, J.; Slugovc, C. *Polymer* **2010**, *51*, 2927. (b) Suthasupa, S.; Shiotsuki, M.; Sanda, F. *Polym. J.* **2010**, *42*, 905. (c) Liu, X.; Basu, A. J. *Organomet. Chem.* **2006**, *691*, 5148. (d) Xia, Y.; Verduzco, R.; Grubbs, R. H.; Kornfield, J. A. *J. Am. Chem. Soc.* **2008**, *130*, 1735.
- (5) For a discussion of the use of metathesis catalysts in natural product synthesis, see: Cossy, J.; Arseniyadis, S.; Meyer, C. *Metathesis in Natural Product Synthesis: Strategies, Substrates, and Catalysts*, 1st ed.; Wiley-VCH: Weinheim, Germany, 2010.
- (6) (a) Binder, J. B.; Raines, R. T. *Curr. Opin. Chem. Biol.* **2008**, *12*, 767. (b) Matson, J. B.; Grubbs, R. H. *J. Am. Chem. Soc.* **2008**, *130*, 6731. (c) Lin, Y. A.; Chalker, J. M.; Davis, B. G. *J. Am. Chem. Soc.* **2010**, *132*, 16805.
- (7) Schrodi, Y.; Ung, T.; Vargas, A.; Mkrtumyan, G.; Lee, C. W.; Champagne, T. M.; Pederson, R. L.; Hong, S. H. *Clean: Soil, Air, Water* **2008**, *36*, 669.
- (8) (a) Casey, C. P.; Tuinstra, H. E.; Saeman, M. C. *J. Am. Chem. Soc.* **1976**, *98*, 608. (b) McGinnis, J.; Katz, T. J.; Hurwitz, S. *J. Am. Chem. Soc.* **1976**, *98*, 605. (c) Casey, C. P.; Tuinstra, H. E. *J. Am. Chem. Soc.* **1978**, *100*, 2270. (d) Lee, J. B.; Ott, K. C.; Grubbs, R. H. *J. Am. Chem. Soc.* **1982**, *104*, 7491. (e) Tanaka, K.; Takeo, H.; Matsumura, C. *J. Am. Chem. Soc.* **1987**, *109*, 2422. (f) Handzlik, J. *J. Mol. Catal. A: Chem.* **2004**, *218*, 91.
- (9) Stewart, I. C.; Keitz, B. K.; Kuhn, K. M.; Thomas, R. M.; Grubbs, R. H. *J. Am. Chem. Soc.* **2010**, *132*, 8534.
- (10) Thomas, R. M.; Keitz, B. K.; Champagne, T. M.; Grubbs, R. H. *J. Am. Chem. Soc.* **2011**, *133*, 7490.
- (11) (a) Meek, S. J.; Malcolmson, S. J.; Li, B.; Schrock, R. R.; Hoveyda, A. H. *J. Am. Chem. Soc.* **2009**, *131*, 16407. (b) Flook, M. M.; Ng, V. W. L.; Schrock, R. R. *J. Am. Chem. Soc.* **2011**, *133*, 1784.
- (12) (a) Sanford, M. S.; Love, J. A.; Grubbs, R. H. *J. Am. Chem. Soc.* **2001**, *123*, 6543. (b) Love, J. A.; Sanford, M. S.; Day, M. W.; Grubbs, R. H. *J. Am. Chem. Soc.* **2003**, *125*, 10103.
- (13) (a) Hong, S. H.; Day, M. W.; Grubbs, R. H. *J. Am. Chem. Soc.* **2004**, *126*, 7414. (b) Courchay, F. C.; Sworen, J. C.; Ghiviriga, I.; Abboud, K. A.; Wagener, K. B. *Organometallics* **2006**, *25*, 6074. (c) Hong, S. H.; Wenzel, A. G.; Salguero, T. T.; Day, M. W.; Grubbs, R. H. *J. Am. Chem. Soc.* **2007**, *129*, 7961.
- (14) (a) Wenzel, A. G.; Grubbs, R. H. *J. Am. Chem. Soc.* **2006**, *128*, 16048. (b) Romero, P. E.; Piers, W. E. *J. Am. Chem. Soc.* **2007**, *129*, 1698. (c) Wenzel, A. G.; Blake, G.; VanderVelde, D. G.; Grubbs, R. H. *J. Am. Chem. Soc.* **2011**, *133*, 6249.
- (15) (a) Romero, P. E.; Piers, W. E.; McDonald, R. *Angew. Chem., Int. Ed.* **2004**, *43*, 6161. (b) Rowley, C. N.; van der Eide, E. F.; Piers, W. E.; Woo, T. K. *Organometallics* **2008**, *27*, 6043. (c) van der Eide, E. F.; Romero, P. E.; Piers, W. E. *J. Am. Chem. Soc.* **2008**, *130*, 4485. (d) Leitao, E. M.; van der Eide, E. F.; Romero, P. E.; Piers, W. E.; McDonald, R. *J. Am. Chem. Soc.* **2010**, *132*, 2784.
- (16) Ruthenacycles have been studied quite extensively in the gas phase. See: (a) Hinderling, C.; Adlhart, C.; Chen, P. *Angew. Chem., Int. Ed.* **1998**, *37*, 2685. (b) Adlhart, C.; Hinderling, C.; Baumann, H.; Chen, P. *J. Am. Chem. Soc.* **2000**, *122*, 8204.
- (17) van der Eide, E. F.; Piers, W. E. *Nat. Chem.* **2010**, *2*, 571.
- (18) Although it would have been advantageous to access ruthenacycles directly from the bispyridine adduct of **5**, a technique demonstrated in ref 14b, we found that such a complex could not be isolated as a single clean species (see the SI).
- (19) Carlson, R. G.; Gile, M. A.; Heppert, J. A.; Mason, M. H.; Powell, D. R.; VanderVelde, D.; Vilain, J. M. *J. Am. Chem. Soc.* **2002**, *124*, 1580.
- (20) Unfortunately, while the resonances corresponding to the ruthenacycle protons were well-resolved, other ligand peaks could not be cleanly identified, most likely because some decomposition took place during the reaction, as evidenced by the relatively low yield of ruthenacycle.
- (21) Sandström, J. *Dynamic NMR Spectroscopy*; Academic Press: New York, 1982; pp 53–54.
- (22) Complete conversion to ruthenacycle **17** from **14** was never observed, even after extended periods of time at ca.  $-40$  °C. Attempts to raise the temperature resulted in decomposition of **17**.
- (23) (a) Anderson, D. R.; Lavallo, V.; O'Leary, D. J.; Bertrand, G.; Grubbs, R. H. *Angew. Chem., Int. Ed.* **2007**, *46*, 7262. (b) Anderson, D. R.; Ung, T. A.; Mkrtumyan, G.; Bertrand, G.; Grubbs, R. H.; Schrodi, Y. *Organometallics* **2008**, *27*, 563.
- (24) The low-yielding synthesis of catalysts of type **10** hampered our ability to examine the behavior of **13** and **14** exhaustively.
- (25) Several smaller peaks that could correspond to structural analogues of **4** are also visible in Figure 2. However, because of the extremely low intensity of these resonances, we can only speculate about their identity.
- (26) Roberts, J. *ABCs of FT-NMR*; University Science Books: Sausalito, CA, 2000; p 61.
- (27) The presence of  $^{13}\text{C}$ -**1** was also confirmed by high-resolution mass spectrometry (HRMS) (FAB+: calcd,  $m/z$  242.1429; found, 242.1471) after the reaction mixture was warmed to room temperature.
- (28) Another structure consistent with all of the spectroscopic data would be an isomer of **19**. However, the large difference in the reactivities of **19** and **22** with excess ethylene leads us to believe that this is probably not the case.
- (29) Direct conversion of **22** into **15** would require generation of a ruthenium methylenide (**21**) and the release of **23** (dashed arrows in Scheme 8). However, neither species was detected by  $^1\text{H}$  NMR spectroscopy or HRMS, suggesting that **22** prefers to give an alkylidene that subsequently reacts with ethylene to give **15**.
- (30) Complex Pathway Simulator (COPASI): Hoops, S.; Sahle, S.; Gauges, R.; Lee, C.; Pahle, J.; Simus, N.; Singhal, M.; Xu, L.; Mendes, P.; Kummer, U. *Bioinformatics* **2006**, *22*, 3067.

(31) Notably, our model relies not on the positive identification of **22** but only on the existence of an equilibrium involving **19** and another ruthenacycle complex.

(32) At longer reaction times, where the change in concentration of **22** was relatively insignificant and the primary reaction consuming **19** is step 1 (rate constant  $k_1$ ), the  $k_{\text{obs}}$  values from a log plot and  $k_1$  values obtained from modeling were generally in good agreement (within a factor of 2 or less).

(33) For a discussion of the kinetic favorability of ring closing, see ref 17.